BIOCHIP JOURNAL, Vol. 2, No. 3, 186-191, September 2008

Continuous Micro-Magnetophoretic Separation using a Dipole Magnetic Field

Oh-Taek Son[1], Jong Wook Roh[2], Suk-Heung Song[1], Jae-Sung Park[1], Wooyoung Lee[2] & Hyo-Il Jung[1]

[1]School of Mechanical Engineering, Yonsei University, 134 Sinchon, Seoul 120-749, Korea
[2]Department of Materials Science and Engineering, Yonsei University, 134 Sinchon, Seoul 120-749, Korea
Correspondence and requests for materials should be addressed to H.-I. Jung (uridle7@yonsei.ac.kr), W. Lee (wooyoung@yonsei.ac.kr)

Accepted 30 July 2008

Abstract

The use of a dipole magnetic field on particle separation in a microfluidic channel is introduced. We compare a monopole magnetic field with a dipole magnetic field by computer simulation, and the separation of magnetic beads utilizing the dipole magnetic field is demonstrated. The dipole field generates a higher magnetic flux density at the separation zone than the monopole field. In the demonstration, the dipole field successfully derives the deflection of magnetic beads flowing through a microfluidic channel.

Keywords: Magnetophoretic separation, Microfluidic channel, Dipole magnetic field, Flow cytometry, Biochip technology

Introduction

In clinical areas, the separation of cells has played a major role in cell research and therapies such as cancer diagnosis, genetic engineering, cell transplantation, and immunology. Until now, macro-sized cell sorting machines have had fundamental applications in these areas. Among them, fluorescence activated cell sorting (FACS) and magnetically activated cell sorting (MACS) have been the most commonly used techniques. However, conventional flow cytometry techniques demand heavy instrumentation and are not applicable on the micro-scale[1]. Even though the accuracy and throughput of these tools are high, experimental demands usually far surpass their capabilities. In other words, they are not appropriate to a single-cell assay[2].

Recently, numerous researches pertaining to micro-sized microfluidic cell sorting devices have been reported. These devices possess remarkable advantages in minimizing the time and cost associated with a routine biological analysis while improving reproducibility[3]. Microfluidic cell sorting schemes based upon fluorescent labeling[4-7], electrophoresis[8], dielectrophoresis[9-11], and magnetophoresis[1,12,13] have been devised. Microfluidic fluorescence activated cell sorting (μ-FACS) is a miniature version of the conventional flow cytometry system of FACS, and it feathers the multi-labeling of cells and an innate accuracy as, except for the microfluidic sample transport system, it shares the same process of FACS. However, the cost and size of optical instrumentation have been regarded as an obstacle. Dielectrophoresis and electrophoresis use a small variation in the movement of cells stemming from the difference of electrical properties. Although they require a source current and electrodes on the chip-cytometer, they have been good candidates in microfluidic cell sorting devices since they can operate without a labeling process.

Apart from the previously mentioned methods, microfluidic magnetically-activated cell sorting (μ-MACS) does not need any optical instrumentation or a current source and electrode. Using an electromagnet or permanent magnet, μ-MACS attracts magnetically-labeled cells in a microfluidic channel. While this method is suitable to make a compact device, prediction and control of the magnetic field are a drawback. For a precise conformation of the magnetic field, a quadrupole magnetic field was applied in a macro-scale cell sorter[14], but it was not applicable in a microfluidic system due to its geometrical restriction; that is, a microfluidic channel is fabricated in a 2-dimensional geometry. To overcome this problem, a new method using ferromagnetic materials placed in a microchannel has been presented, which requires a bothersome deposition process[15-17].

In this paper, we present an interesting μ-MACS scheme that can control and enhance the deflection of particles by forming a dipole magnetic field with two permanent magnets perpendicular to the microfluidic channel.

Results and Discussion

Mechanism of Magnetophoretic Separation

Figure 1 illustrates a schematic diagram of the di-

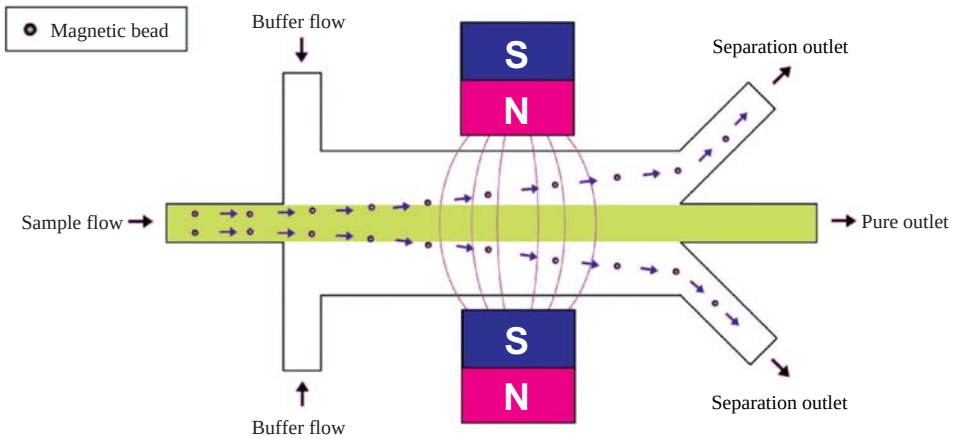

Figure 1. A schematic diagram of the dipole magnet sorter used in the experiment.

pole magnet sorter. Two magnets sit face-to-face and enhance the field strength. Magnetic beads are released from a sample inlet and are deflected by the magnetic attraction. Finally, they are separated from the center flow area colored with green and go through separation outlets. In a microfluidic environment, the inertia and gravitational effects are negligible because of the small volume of the particle[18]. Also, microparticles traveling in the microlfuidic channel are affected by a drag force due to the high surface-to-volume ratio. Therefore, the forces exerted on a magnetic particle flowing through the microfluidic channel consist of a magnetic force and viscous drag force.

The magnetic force is calculated using the following equation:

$$\vec{F}_{magnetic} = V\Delta\chi \frac{\nabla \vec{B}^2}{2\mu_0}, \quad (1)$$

where V is the volume of a magnetic particle, $\Delta\chi$ is the volumetric susceptibility relative to the medium, $\vec{B}$ is the magnetic flux density, and μ_0 is the permeability of free space[19]. When a particle migrates due to a magnetic force, a drag force is inevitably generated as a reaction. The drag force is generally proportional to the magnitude of velocity. The magnetic force exceeds the drag force at the initial state; however, soon the drag force catches up with the magnetic force. In a creeping flow with Reynold's numbers of less than unity, the drag force is defined by Stoke's law as shown in the following equation:

$$\vec{F}_{drag} = 6\pi R\eta\vec{v}, \quad (2)$$

where R is the radius of a magnetic particle, η is the dynamic viscosity of the medium, and $\vec{v}$ is the velocity of the magnetic particle. Here, the velocity of the magnetic particle is driven from the equilibrium state of the magnetic and drag forces, as shown in the following equations:

$$\vec{F}_{magnetic} = \vec{F}_{drag}, \quad (3)$$

$$V\Delta\chi \frac{\nabla \vec{B}^2}{2\mu_0} = 6\pi R\eta\vec{v}, \text{ and} \quad (4)$$

$$\vec{v} = \frac{2R^2\Delta\chi}{9\eta} \nabla\left(\frac{\vec{B}^2}{2\mu_0}\right). \quad (5)$$

In magnetophoretic cell separation, the deflection of a magnetic bead from the initial flow path is applied to sort the target particle. In this case, the particle traveling distance in a perpendicular direction to the flow direction is of interest. If the magnetic field is actuated in x-direction, the traveling distance is calculated by the next equation:

$$\Delta x = v_x t = \frac{2R^2\Delta\chi}{9\eta} \nabla\left(\frac{B_x^2}{2\mu_0}\right) t, \quad (6)$$

where t is the time taken for the magnetic bead to pass through the magnetic field's actuated zone. The actuated time is inversely proportional to the flow rate. Equation (6) shows that the deviation from the initial path is proportional to the gradient of the magnetic flux density squared and time t. By adjusting the two variables, it is possible to control the migration of magnetic beads in a microfluidic channel.

Comparison between a Monopole Field and a Dipole Field

The deviation of a magnetic particle from its initial path is proportional to the gradient of the magnetic flux density squared; thus, it is inversely proportional to the distance squared by the inverse square law. If two magnets are aligned in-parallel, magnetic lines from the N-pole do not need to go toward the S-pole locating at the back-side of the magnet, but go direct-

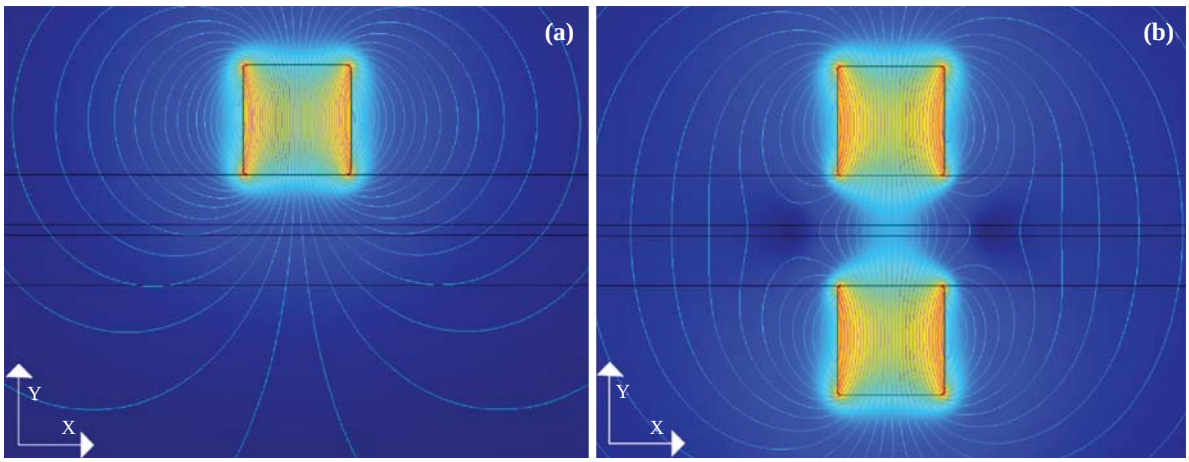

Figure 2. Simulation of the magnetic fields of (a) monopole and (b) a dipole magnetic systems.

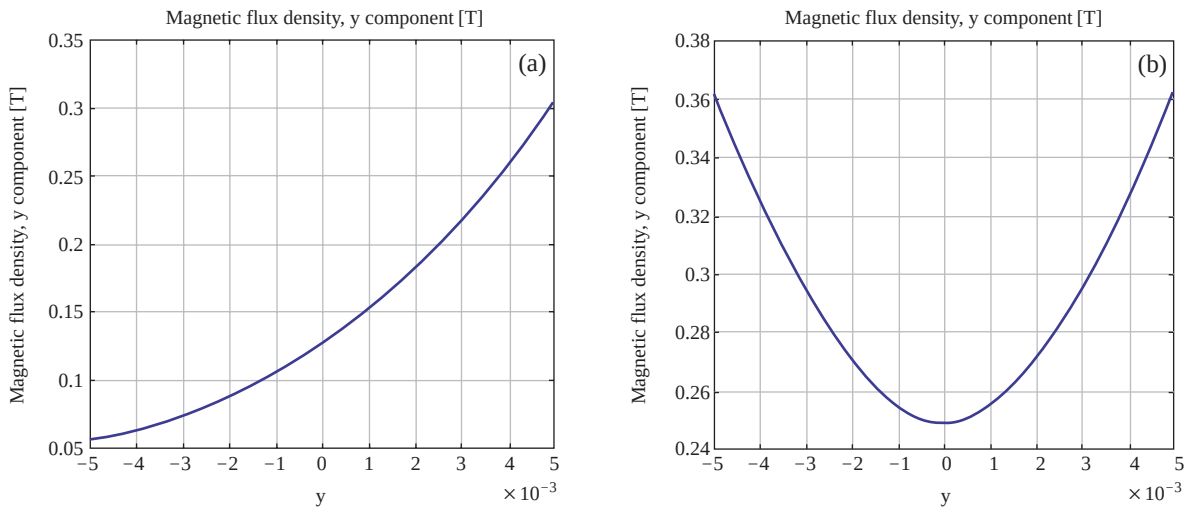

Figure 3. The variation of magnetic flux density across the microchannel in (a) monopole and (b) dipole magnetic fields.

ly to the S-pole confronting it. As a result, the dipole field can prevent the loss of magnetic flux density in the microfludic channel residing at some distance from the magnet.

We examined the difference in magnetic flux density between monopole magnet and dipole magnet using a simulation method. The actual magnetic flux density of the permanent magnet (Nd-Fe-B) was measured with a Gauss meter (Gauss/Tesla meter model 5080, SYPRIS Co.) and was used in the simulation. A computer simulation of the magnetic field was conducted using COMSOL Multiphysics Ver. 3.3 (COMSOL Inc.), which is widely adopted in electromagnetic field simulation. Figure 2 presents the magnetic field lines of a monopole field and dipole field. The monopole magnet shows a closed loop in the magnetic field spreading at the microchannel region, while the dipole magnet system shows a more concentrated magnetic field. The specific magnetic flux density variation across the channel is presented in Figure 3. The magnetic flux density of the monopole magnet gradually decreases to 0.125 at the channel region (Figure 3a), but that of the dipole magnet is 0.25 as there is a recovery at the position between the two magnets resulting in a rise to the initial strength (Figure 3b).

In a channel area having a small dimension, the gradient of magnetic flux density along the perpendicular direction is negligible, so only the horizontal gradient of magnetic flux density is of importance[20].

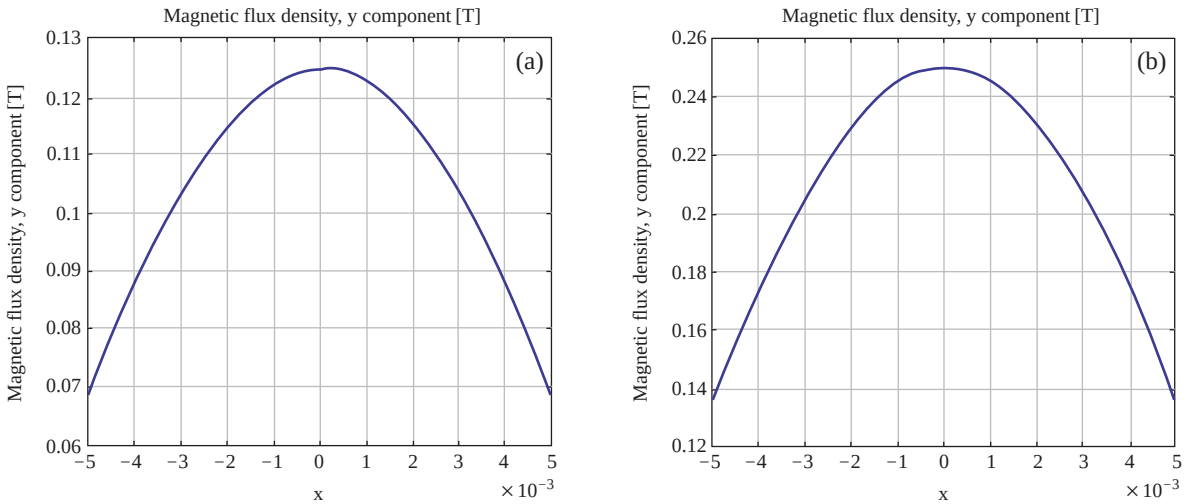

Figure 4. The variation of magnetic flux density along the microchannel in (a) monopole and (b) dipole magnetic fields.

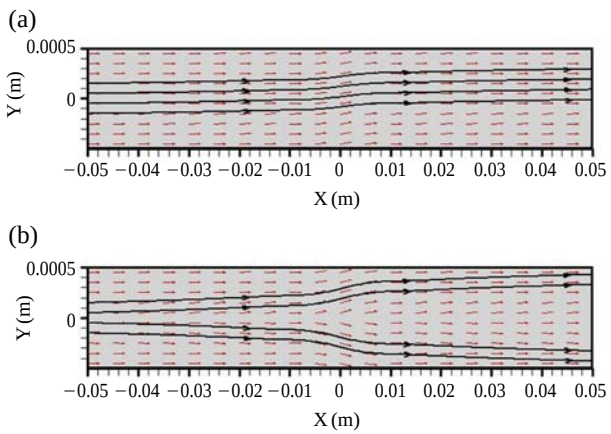

Figure 5. A simulation of the deflection of particles in the microchannel by (a) monopole and (b) dipole fields.

As shown in Figure 4, nevertheless the morphology of the graphs are similar, and the magnetic flux density of the monopole field along the horizontal direction ranges from 0.068 T to 0.125 T, while that of the dipole field ranges from 0.135 T to 0.25 T. In conclusion, we can certify that the dipole magnet exerts a larger amount of force than the monopole magnet.

Demonstration of the Dipole Magnet Sorter

Prior to the experimental confirmation of magnetic bead separation, we simulated the deflection of magnetic particles in both the monopole and dipole magnetic fields. In the simulation, the applied parameters of the microchannel dimension, flow speed, particle size, and magnetic flux density were identical to the experimental conditions. Figure 5 shows the vector fields and path lines indicating the migration of particles ejected from a sample inlet in the microchannel. By looking at the path lines, we could presume that the particle traveling distance (Δx) would be ~120 and ~280 μm in the monopole and dipole fields, respectively. The high degree of deflection was a definite result owing to the intensified magnetic flux density formed in the dipole field.

In the demonstration of particle separation, the dipole magnet showed a strong magnetic attraction on the magnetic bead passing through the microfluidic channel, and the optimal flow speed for the full separation was remarkably higher (42 mm/s) than the monopole magnet (around 20 mm/s). The advantage of lab-on-a-chip is the increase of accuracy, regarded as applicable in single-cell analysis. However, this high accuracy possessed another consideration that the analysis should allow a low throughput. The dipole magnet sorter will enhance the speed of analysis in a micro MACS system. In further research, the magnetic field of a dipole magnet will be analyzed in a 3-dimensional system, and a cell magnetically labeled will be tested using this scheme.

Conclusion

On-chip separation of magnetic beads using a dipole magnetic field was demonstrated. The magnetic fields of a monopole magnet and a dipole magnet were analyzed by computer simulation software, COMSOL multiphysics 3.3. The dipole magnet showed a concentrated magnetic field profile on the separation area, and the gradient of magnetic flux density was higher than the monopole magnet. In the real experiment,

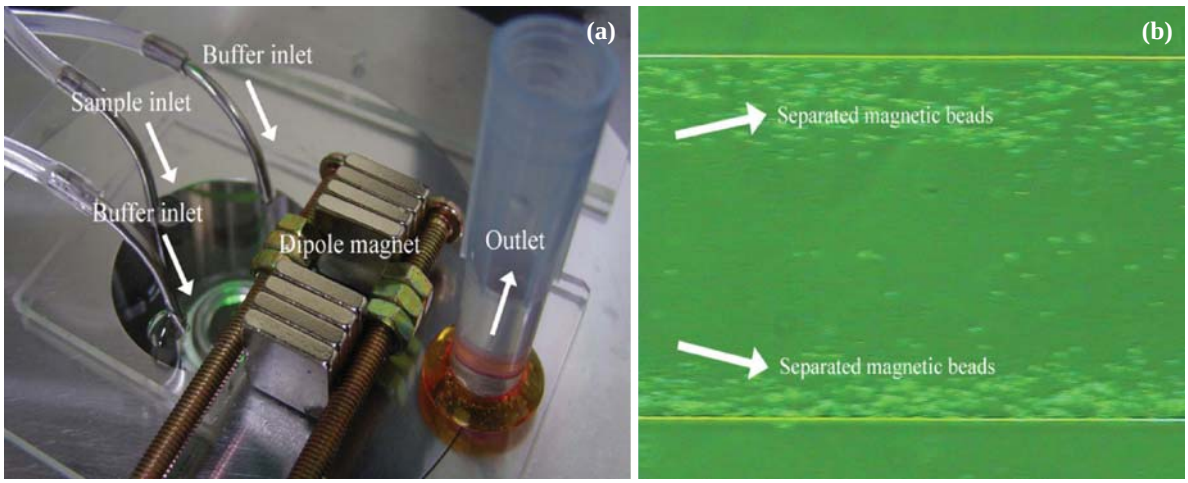

Figure 6. Photographs of (a) experimental setup using the dipole field and (b) separation of magnetic beads.

the dipole field successfully demonstrated the particle separation in a microfluidic channel.

Materials and Methods

Fabrication and Experimental Setup

To make a microfluidic channel identical to the geometry shown in Figure 1, a conventional fabrication method of PDMS soft-lithography was applied[21]. An epoxy-based negative photoresist (SU-8 2025, MicroChem) was applied to fabricate a microfluidic channel of 30 μm height and 1 mm width. After preparing the SU-8 mold on a silicon wafer, we then poured the PDMS gel mixture (DC 184-A : B=9 : 1, Dow Corning) onto the SU-8 mold. After curing the PDMS, the PDMS microfluidic channel was peeled off from the SU-8 master, and it was then treated with O2 plasma for permanent bonding with a glass substrate[22]. After the plasma bonding, de-ionized water was immediately injected to maintain the microfluidic channel in its hydrophilic state. Three syringes were connected with each inlet of the microfluidic channel, actuating a microflow of Dynabeads M-280 streptavidin (Invitrogen Inc.) through the channel by utilizing syringe pumps (KD Scientific, KD-560). The motion of the magnetic beads was recorded by a CCD camera via an inverted microscope (IX 71, Olympus). We used two permanent magnets aligned in-parallel to conform the dipole magnetic field. A picture of the experimental setup is represented in Figure 6a. With a flow rate of 75 μL/min corresponding to a mean velocity of 42 mm/s, the separation of magnetic beads was successfully demonstrated (Figure 6b).

Acknowledgements

This work was due to a grant from a program of KOSEF through the National Core Research Center for Nanomedical Technology (R15-2004-024-00000-0), Seoul Research and Business Development Program (10816), and Korea Research Foundation (MOEHRD, KRF-2005-042- D00203).

References

1. Pamme, N. & Wilhelm, C. Continuous sorting of magnetic cells via on-chip free-flow magnetophoresis. *Lab. Chip* **6**, 974-980 (2006).
2. Robert, W. *et al*. Microfluidic sorting system based on optical waveguide integration and diode laser bar trapping. *Lab Chip* **6**, 422-426 (2006).
3. Mitchell, P. Microfluidics-downsizing large-scale biology. *Nat. Biotechnol.* **19**, 717-721 (2001).
4. Fu, A.Y., Spence, C., Scherer, A., Arnold, F.H. & Quake, S.R. A microfabricated fluorescence-activated cell sorter. *Nat. Biotechnol.* **17**, 1109-1111 (1999).
5. Krüger1, J. *et al*. Development of a microfluidic device for fluorescence activated cell sorting. *J. Micromech. Microeng.* **12**, 486-494 (2002).
6. Yao, B. A microfluidic device based on gravity and electric force driving for flow cytometry and fluorescence activated cell sorting. *Lab Chip* **4**, 603-607 (2004).
7. Yang, S.Y. *et al*. A cell counting/sorting system incorporated with a microfabricated flow cytometer chip. *Meas. Sci. Technol.* **17**, 2001-2009 (2006).
8. Xuan, X. & Li, D. Focused electrophoretic motion and selected electrokinetic dispensing of particles and cells in cross-microchannels. *Electrophoresis* **26**,

3552-3560 (2005).
9. Hu, X. *et al*. Marker-specific sorting of rare cells using dielectrophoresis. *PNAS* **102**, 15757-15761 (2005).
10. Doh, I. & Cho, Y.H. A continuous cell separation chip using hydrodynamic dielectrophoresis (DEP) process. *Sensors and Actuators A* **121**, 59-65 (2005).
11. Park, J. *et al*. An efficient cell separation system using 3D-asymmetric microelectrodes. *Lab. Chip* **5**, 1264-1270 (2005).
12. Choi, J.W., Ahn, C.H., Bhansali, S. & Henderson, H.T. A new magnetic bead-based, filterless bio-separator with planar electromagnet surfaces for integrated bio-detection systems. *Sens. Actuator B-Chem.* **68**, 34-39 (2000).
13. Kim, H.S. *et al*. Separation of apoptotic cells using a microfluidic device. *Biotechnol. Lett.* **29**, 1659-1663 (2007).
14. Zborowski, M., Sun, L., Moore, L.R., Williams, P.S. & Chalmers, J.J. Continuous cell separation using novel magnetic quadrupole flow sorter. *J. Magn. Magn. Mater.* **194**, 224-230 (1999).
15. Xia, N. *et al*. Combined microfluidic-micromagnetic separation of living cells in continuous flow. *Biomed. Microdevices* **8**, 299-308 (2006).
16. Hahn, Y.K. *et al*. Magnetophoretic immunoassay of allergen-specific IgE in an enhanced magnetic field gradient. *Anal. Chem.* **79**, 2214-2220 (2007).
17. Siegel, A.C. *et al*. Cofabrication of electromagnets and microfluidic systems in Poly(dimethyl-siloxane). *Angew. Chem. Int. Ed.* **45**, 1-6 (2006).
18. Ramadan, Q., Samper, V., Poenara, D. & Yu, C. On-chip micro-electromagnets for magnetic-based biomolecules separation. *J. Magn. Magn. Mater.* **281**, 150-172 (2004).
19. Zborowski, M., Fuh, C.B., Green, R., Sun, L. & Chalmers, J.J. Analytical magnetapheresis of ferritin-labeled lymphocytes. *Anal. Chem.* **67**, 3072-3712 (1995).
20. Moore L.R., Zborowski, M., Sun, L. & Chalmers, J.J. Lymphocyte fabrication using immuno-magnetic colloid and a dipole magnet flow cell sorter. *J. Biochem. Biophys. Methods* **37**, 11-33 (1998).
21. Xia, Y. & Whitesides, G.M. Soft lithography. *Angew. Chem. Int. Ed.* **37**, 550-575 (1998).
22. Bhattacharya, S., Datta, A., Berg, J.M. & Gangopadhyay, S. Studies on surface wettability of poly (di-Methyl) siloxane (PDMS) and glass under oxygen-plasma treatment and correlation with bond strength. *J. Microelectromechanical Sys.* **14**, 590-597 (2005).